Volatile Anesthetic Binding to Proteins Is Influenced by Solvent and Aliphatic Residues

John H. Streiff* and Keith A. Jones

Department of Anesthesiology, University of Alabama at Birmingham, 901 19th Street South, Birmingham, Alabama 35294-1150

Received June 16, 2008

The main objective of this work was to characterize VA binding sites in multiple anesthetic target proteins. A computational algorithm was used to quantify the solvent exclusion and aliphatic character of amphiphilic pockets in the structures of VA binding proteins. VA binding sites in the protein structures were defined as the pockets with solvent exclusion and aliphatic character that exceeded minimum values observed in the VA binding sites of serum albumin, firefly luciferase, and apoferritin. We found that the structures of VA binding proteins are enriched in these pockets and that the predicted binding sites were consistent with experimental determined binding locations in several proteins. Autodock3 was used to dock the simulated molecules of 1,1,1,2,2-pentafluoroethane, difluoromethyl 1,1,1,2-tetrafluoroethyl ether, and sevoflurane and the isomers of halothane and isoflurane into these potential binding sites. We found that the binding of the various VA molecules to the amphiphilic pockets is driven primarily by VDW interactions and to a lesser extent by weak hydrogen bonding and electrostatic interactions. In addition, the trend in $\Delta G_{\text{binding}}$ values follows the Meyer-Overton rule. These results suggest that VA potencies are related to the VDW interactions between the VA ligand and protein target. It is likely that VA bind to sites with a high degree of solvent exclusion and aliphatic character because aliphatic residues provide favorable VDW contacts and weak hydrogen bond donors. Water molecules occupying these sites maintain pocket integrity, associate with the VA ligand, and diminish the unfavorable solvation enthalpy of the VA. Water molecules displaced into the bulk by the VA ligand may provide an additional favorable enthalpic contribution to VA binding. Anesthesia is a component of many health related procedures, the outcomes of which could be improved with a better understanding of the molecular targets and mechanisms of anesthetic action.

INTRODUCTION

Anesthesia is ultimately the manifestation of volatile anesthetic (VA) effects on protein function in complex biological systems. The minimum alveolar concentration (MAC), which is the EC_{50} value of the concentration dependence of VA inhibition of mobility in response to a noxious stimulus, is a measure of the potency of an anesthetic, and it correlates with the oil gas partition coefficient (Pog) of the anesthetic. This correlation, known as the Meyer-Overton rule, indicates that VA potency increases with hydrophobicity and suggests that anesthesia is transduced through hydrophobic domains. Classically this was interpreted to be membranes, but the contemporary view favors interactions with hydrophobic domains in proteins, primarily those associated with the membrane. Although membrane association is not a requisite for VA effects because the potencies (ED_{50} values) of various VA agents on the function of firefly luciferase, assayed in the absence of lipid, follow the Meyer-Overton rule.[1] Thus, anesthesia may result from VA binding to hydrophobic sites in proteins.

The few high resolution structures of VA-protein complexes determined to date demonstrate that VA molecules bind to amphiphilic pockets without perturbing the native protein structure. Statistical analysis of the residues surrounding these sites indicates that VA binding correlates with the solvent exclusion and number of methyl containing side chains but not the numbers of residues containing aromatic, sulfur, alcohol, acid, base, or amide groups.[2] This finding suggests that VA binding is influenced by the water molecules solvating the binding site as well as the methionine, threonine, and aliphatic residues lining the binding site. However, this finding is based on a small sample of protein structures. A goal of this investigation is to determine whether this finding is consistent in a larger sample of protein structures.

Computational approaches offer the only tractable techniques for resolving the individual binding sites and binding energies of a variety of VA molecules in a moderately sized set of proteins. Absolute binding energies are calculated most accurately with sophisticated methods such as free energy perturbation,[3] in which the binding energy is a function of the system energies determined from molecular dynamics simulations of the solvated protein−ligand complex and the solvated unbound ligand. Faster, but less accurate, methods use force field parameters and a free energy function to estimate the binding energy of a ligand docked within a protein structure. Hence, docking algorithms are better suited to rank the relative binding energies of ligand-protein interactions. A conventional use for docking is to virtually screen libraries of small molecules for binding in a protein active site as part of a drug design strategy. A variation on this, termed inverse docking, is a technique to screen a simulated drug for binding to a library of protein structures.[4]

* Corresponding author phone: (205)934-7707; fax: (205)934-7447; e-mail: jstreiff@uab.edu.

10.1021/ci800206a CCC: $40.75
Published on Web 09/23/2008

Table 1. Details of VA

compound	common name	formula	torsions	μD	Pog	MAC (atm)
2-bromo-2-chloro-1,1,1-trifluoroethane	halothane	C_2BrClF_3H	1	1.9−1.6	220[a]	0.009[44]
1,1,1,2,2-pentafluoroethane		C_2F_5H	1	0.45	1.52[45]	1.51[45]
1-chloro-2,2,2-trifluoroethyl difluoromethyl ether	(R) isoflurane	$C_3ClF_5H_2O$	3	1.1	90.8[b]	0.0169[19]
	(S) isoflurane			2.3		0.0144[19]
difluoromethyl 1,1,1,2- tetrafluoroethyl ether		$C_3F_6H_2O$	3	1.0	17.9[46]	0.078[46]
2,2,2-trifluoro-1-[trifluoromethyl]ethyl fluoromethyl ether	sevoflurane	$C_4H_3F_7O$	4	1.1	50[c]	0.024[44]

[a] Halocarbon Laboratories (River Edge, NJ). [b] Hospira, Inc. (Lake Forrest, IL). [c] Abbott Laboratories (North Chicago, IL).

Docking methods are suited to predicting VA-protein interaction because the few structures of VA-protein complexes that have been determined indicate that VA bind to pre-existing amphiphilic pockets without perturbing the structure of the protein.[5−7] The docking program Autodock3 has been used to determine the binding sites and estimate the dissociation constant (kd) of halothane in the structure of ketosteroid isomerase[8] and firefly luciferase.[9] The results are consistent with experimental findings and indicate that docking can resolve the location and kd of individual VA binding interactions, even in oligomeric protein structure with multiple binding sites. These findings are significant because it is experimentally challenging to resolve individual VA-protein interactions when there are multiple VA binding sites.[10] This suggests that docking is a tool that can deconvolute the binding energies of multiple VA interactions with a single protein and simulate the structures of VA-protein complexes, which is an efficient alternative to experimentally determining the structure of the complex.

The main objective of this work was to characterize the VA binding sites in multiple proteins, which are potential anesthetic targets. We used computational methods to analyze the structures of 38 soluble and membrane proteins, including ion channels and receptors, that are photoaffinity labeled by [^{14}C]halothane.[11,12] We identified approximately 200 putative VA binding sites in the sample, spread throughout an array of protein domains and sequences that capture the diversity in sequence identity that can be considerable even for homologous proteins in multiple organisms. Consequently the results are broadly applicable to mechanisms of VA effects on proteins, regardless of the targets. This study is significant because it generates theoretical structures of VA protein complexes that illustrate the link between the binding of VA to proteins and VA potencies observed in complex biological systems.

MATERIALS AND METHODS

Protein Structures. The structures of VA binding proteins are from the same organism in which VA binding was determined or a homologous protein with sequence identity exceeding 80%. The structures of proteins, for which VA binding has not been experimentally determined, were selected by searching the PDB for proteins from *Homo sapiens* cataloged under the Medical Subject Headings A02.633: Muscles or A08: Nervous System. The molecular viewer VMD[13] and associated software packages were used to add missing hydrogen atoms to protein structures, to insert transmembrane proteins into a simulated POPC lipid bilayer, and to solvate the proteins in a 10 Å layer of simulated water. The molecular dynamics package NAMD[14] was used to energy minimize the simulated structures. Protein structures, which were determined as components of multisubunit complexes, are prepared as the complex; however, only the water, lipids, and protein residues within 10 Å of the protein subunits of interest were minimized and used in subsequent calculations.

Identifying Amphiphilic Pockets in Protein Structures. Binding site predictions (BSP) in the protein structures are determined using a geometric algorithm (PASS) to identify potential binding sites for small hydrophobic molecules, such as drug precursors.[15] PASS fills defects in the protein packing with virtual spheres of radius 1−0.7 Å. Each virtual sphere is assigned a burial count, which is equal to the total number of heavy protein atoms (N, C, O, S) within 8 Å, and a weight, which is the summation of the burial counts of neighboring spheres multiplied by an envelope function that decays to zero at a distance of 4.5 Å from the center of the sphere. Thus, the weight of a particular sphere quantifies the local protein structure and increases the more deeply the virtual sphere is buried. PASS assumes that the solvent accessibility of a site within a protein is inversely proportional to the weight of the virtual spheres located in that site. In other words, as the weight increases the solvent accessibility decreases, which makes the site better suited for sequestering hydrophobic ligands (hydrophobic effect). In addition, we quantify the aliphatic character of each site using a methyl burial count and a methyl weight, which are calculated using the above functions except substituting the number methyl hydrogen atoms for total protein atoms. The rationale for this comes from NMR experiments, which demonstrate that halothane contacts predominantly aliphatic and aromatic residues in HSA[16] and the VA methoxyflurane exclusively contacts the choline methyl group in dipalmitoylphosphatidylcholine micelles.[17] Those sites with solvent exclusion (weight) and numbers of methyl hydrogen atoms (methyl weight), which exceed threshold values determined from the structures of VA-protein complexes, are designated as BSP.[2] Thus, the BSP are located in sites that share common chemical motifs with VA binding sites, namely amphiphilic pockets with limited solvent accessibility.[18]

Ligand Structures. A series of VA molecules with a range of potencies on the Meyer-Overton continuum (Table 1) are investigated in this work. Sevoflurane, halothane, and isoflurane are used because of their clinical applications as general anesthetics. Although the use of halothane is being discontinued, it has the most empirical binding data in the literature from which to draw comparisons to results of docking predictions. Isoflurane and halothane, which are usually administered as racemic mixtures, are resolved into (R) and (S) isomers because there are slight differences

between the potencies of isoflurane enantiomers in rats[19] and the kinetics of isoflurane enantiomers binding to serum albumin.[20] Also included are the molecules 1,1,1,2,2-pentafluoroethane (NHL) and 1,1,1,2-tetrafluoroethyl difluoromethyl ether (NFL), which are lower potency analogs of halothane and isoflurane, respectively. The program PRODRG[21] was used to prepare topology files for the VA molecules. PRODRG employs the empirical GROMOS87 force field to generate accurate geometries of small molecules.[22]

Predicting VA Binding Energies. The binding energies and geometries of the VA are calculated using Autodock3, which utilizes a grid based algorithm to calculate a free energy function, $\Delta G = \Delta G_{vdw} + \Delta G_{Hbond} + \Delta G_{elec} + \Delta G_{tor} + \Delta G_{sol}$.[23] The dispersion repulsion term, ΔG_{vdw}, is calculated using parameters adapted from the AMBER force field[24] and yields energies down to -0.2 kcal/mol for each favorable atom-atom contact. The hydrogen bonding term, ΔG_{Hbond}, is modeled with a directional Leonard-Jones 12−10 potential that yields no change in free energy for ligands with the same number of hydrogen bonds in the complex as in solution. The electrostatic term, ΔG_{elec}, is modeled with a screened coulomb potential weighted to yield an energy of -1.0 kcal/mol for an ideal salt bridge. The restriction of the ligand's internal rotors and global rotation translation is modeled by the ΔG_{tor} term, which yields an energy of about 0.3 kcal/mol for each torsional degree of freedom in the ligand. The solvation term, ΔG_{sol}, yields approximately -0.2 kcal/mol for each aliphatic carbon in the ligand buried in the protein. The VA molecules lack polar atoms and strong hydrogen bond donors or acceptors so ΔGvdw is the dominant enthalpic term of the free energy function. The ligand poses are scored using the docked energy, which is the sum of the inter- and intramolecular interaction energies. The binding energy ($\Delta G_{binding}$) of the ligand is calculated from the sum of the intermolecular and torsional free energies. The binding energy and dissociation constant are related through the expression $\Delta G_{binding} = -RT \ln(kd)$, where R is the gas constant 1.987 kcal/mol, and the temperature T is taken to be 300 K.

The package Autodock tools[25] is used to reformat the minimized protein structures for input into Autodock3. The simulated molecules of VA compounds are docked in each BSP. Blind docking tester[26] is used to manage the docking trials. A 9 Å^3 grid with 0.1 Å resolution and centered at each BSP is calculated for every protein. Each VA is docked in the grid surrounding the BSP using a genetic algorithm with local search to find the bound VA geometry. Each docking is repeated ten times to ensure that $\Delta G_{docking}$ is independent of starting conditions.

Analysis. The values of ln (kd) calculated for the compounds docked in each BSP are plotted as a function of ln (Pog) and nonlinear least-squares fit to ln (kd) = a*ln (Pog) + b. The means and standard deviations of the slopes (a), y-intercepts (b), and correlation coefficients (R^2) are presented to show that the dissociation constants predicted for these compounds binding to numerous amphiphilic pockets in a multitude of proteins decrease with the oil gas partition coefficient across this series of compounds.

RESULTS

A total of 76 protein structures were analyzed. Details of the protein structures are provided in the Supporting Information. Most of the structures were determined by X-ray crystallography methods and have resolutions that range from 1.7 to 4.1 Å. The remaining structures were determined by either electron crystallography, cryo-EM, or NMR methods. A theoretical model of apolipoprotein A[27] was also used because membrane/lipid interacting proteins are thought to be important targets of VA and are under-represented in the protein data bank. Thirty-four of the structures are completely ordered. Twenty-nine of the structures have disordered segments at just one or both termini. Twenty-two structures have disordered segments at various locations within their sequence, and 16 of these structures also have disordered segments at one or both termini. In all but one structure the disordered segments are short and less than 5% of the protein sequence. However, the theoretical model of apolipoprotein A1 is missing the first 48 residues or approximately 25% of its sequence. In each case, the disordered segments could indicate dynamic regions of the protein structure. We did not attempt to model missing segments of protein structures because we assume that disordered regions do not form surfaces of pre-existing amphiphilic pockets where VA prefer to bind. However, we did verify that no VA binding sites were located in artificial voids created by missing protein segments. Predicted structures of the VA-protein complexes, for which other groups have resolved VA binding site locations, are presented for the purpose of method evaluation. In Figure 1, the structure of ketosteroid isomerase with (R) halothane docked at five BSP is shown next to the structure of porcine odorant binding protein with sevoflurane docked at the lone BSP. The VA are docked between the ketosteroid isomerase homodimer and within its substrate binding site, which is consistent with a previous docking study,[8] and within the ligand binding site of odorant binding protein about 9 Å from tryptophan 16 and tyrosine 82, which is consistent with the experimental finding that emission from one or both of these residues is quenched by halothane.[28] These proteins are similar in that the VA are predicted to bind to native ligand sites found within domains consisting of predominantly β sheet secondary structure. In Figure 2, the structure of myoglobin with VA docked to a single BSP is shown next to the structure of adenylate kinase with (R) halothane docked to two BSP. The VA are docked to the heme binding site of myoglobin, which is consistent with the finding that VA bind to apomyoglobin, but not myoglobin,[29] and to the nucleotide binding site in adenylate kinase, which is consistent with the finding that halothane binds to the AMP pocket.[30] These two proteins are similar in that the VA are predicted to bind to native ligand sites found in predominantly α-helical domains. In Figure 3, the structure of an apoferritin homodimer with an (R) isoflurane molecule docked in the single interfacial BSP, which agrees with experimental findings,[7] is shown next to the structure of rhodopsin with (R) halothane docked to four BSP, one of which coincides with the retinal pocket where tryptophan 265 is photoaffinity labeled by halothane.[31] These two proteins are similar in that VA molecules are predicted to bind to sites within four α helix bundles, which is a motif found in the transmembrane domains of anesthetic sensitive

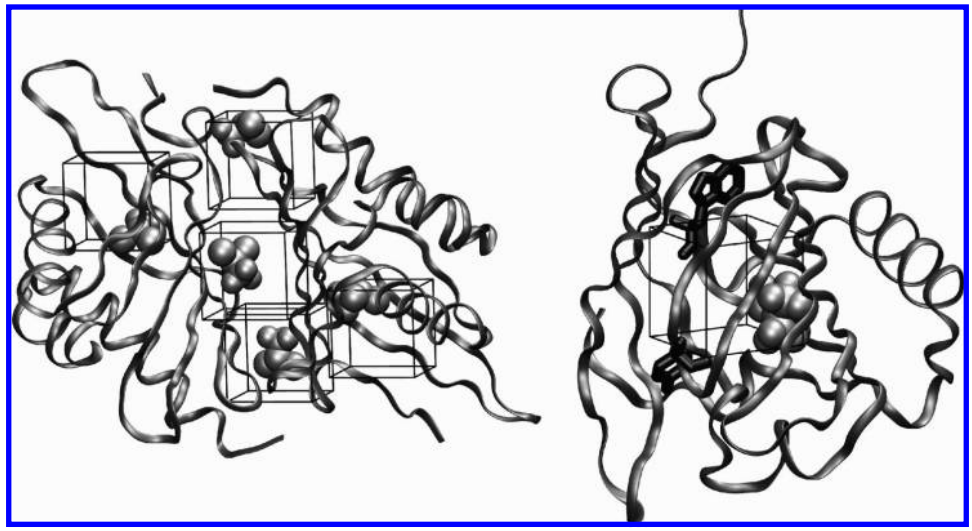

Figure 1. (left) Results of docking (R) halothane (VDW representation) to the structure of ketosteroid isomerase (ribbon representation). (right) Sevoflurane (VDW representation) docked to the structure of odorant binding protein (ribbon representation) nearby tryptophan 16 and tyrosine 82 (black licorice representation). The dimensions of the docking areas are outlined in black.

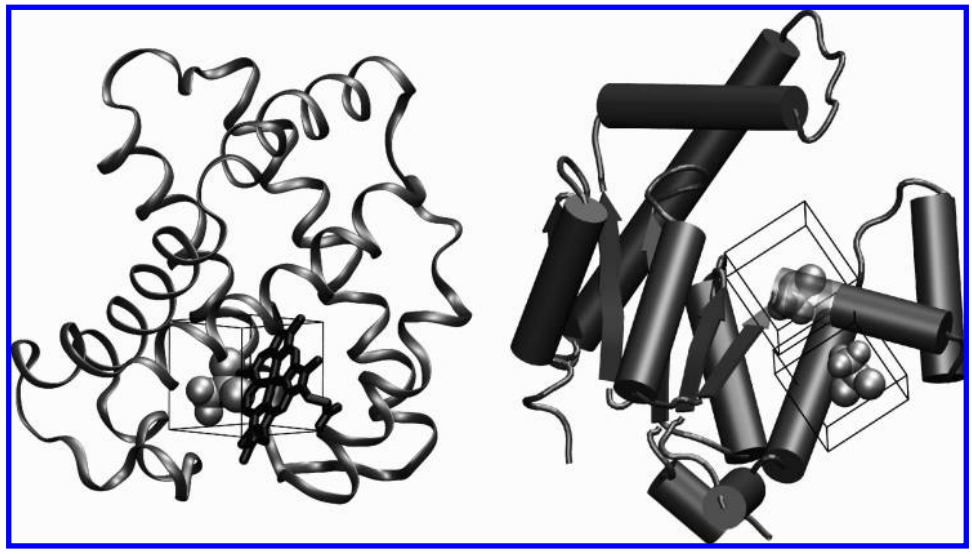

Figure 2. (left) (R) Halothane docked to BSP in the structure of myoglobin overlaps the heme moiety (black licorice representation). (right) (R) Halothane docked to BSP in the structure of adenylate kinase, which is drawn in cartoon representation to match the style and orientation used in the original reference. Residues 38−42 are transparent, so they do not obscure one of the halothane ligands (silver VDW representation).

ion channels. Although the crystal structures of halothane and isoflurane bound to apoferritin have been determined (1XZ1 and 1XZ3, respectively), we docked the VA to a structure of apoferritin determined in the absence of any ligands (1AEW) because it had fewer missing residues.

Predicted and observed $\Delta G_{binding}$ values for certain complexes are listed in Table 2.

The values of ln (MAC) are plotted as a function of ln (Pog) in Figure 4. The mean values (+sd) of ln (kd) are plotted as a function of ln (Pog) in the same graph but using a different scale (right ordinate). The slope of ln (MAC) vs ln (Pog) is approximately −1.0 with a correlation coefficient of 0.98. The mean (±sd) of the slopes of the plots of ln (kd) vs ln (Pog) is -0.30 ± 0.05; the mean of the intercepts is -4.0 ± 0.5, and the mean of the correlation coefficients is 0.9 ± 0.1. We investigated the influence of each VA molecule on the mean of the slopes of ln (kd) vs ln (Pog) by recalculating the slopes using the other six. We found that the slopes of the plots are not strongly dependent on any particular VA molecule. Although the slope of ln (MAC) is almost 3-fold steeper than the mean of ln (kd), both have the same trend.

DISCUSSION

The main finding of this work is that VA binding proteins have amphiphilic pockets with a high degree of solvent exclusion and methyl containing side chains to which a variety of VA molecules dock with $\Delta G_{binding}$ values that trend according to the Meyer-Overton rule. These findings are important because they support hypotheses that VA potency is a function of VA-protein binding.

201 BSP were identified in 37 out of the 38 structures (45 out of 46 unique chains) of proteins to which VA experimentally bind, but only 62 BSP were identified in 24 out of 36 structures (26 out of 38 unique chains) of proteins without experimental evidence of VA binding. This indicates that BSP are found in many proteins yet are enriched in VA

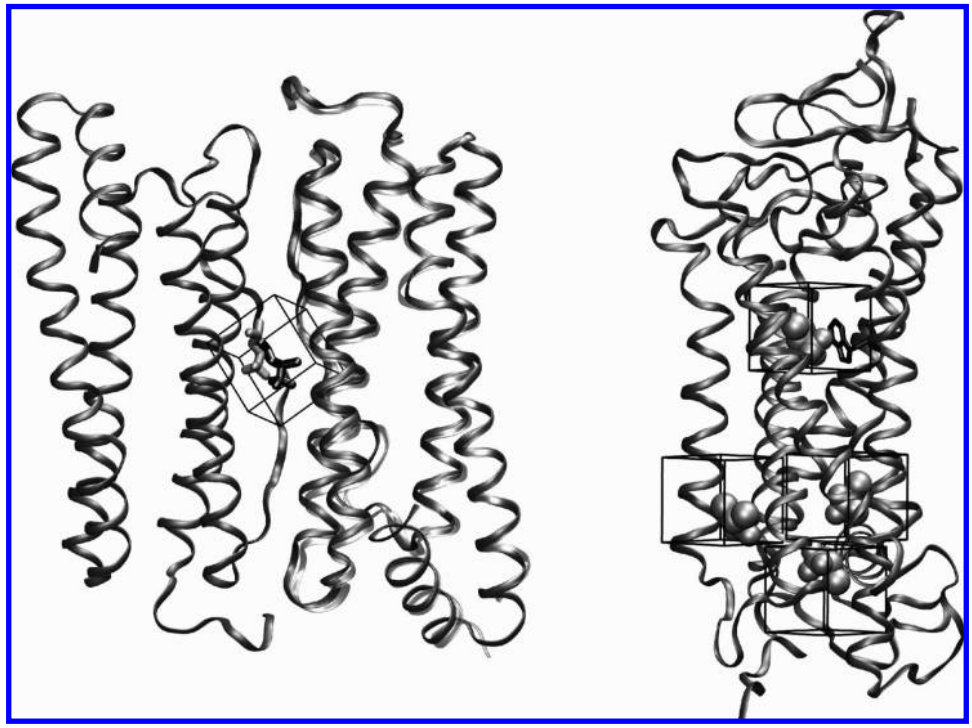

Figure 3. (left) Results of docking (R) isoflurane (silver licorice representation) at the interface between apoferritin homodimer (gray ribbon representation). The structure of 1XZ3 monomer (transparent ribbon) and isoflurane molecules (black licorice representation) are overlaid to show the rmsd of the protein alignment and docked isoflurane. (right) (R) Halothane docked to BSP in the structure of rhodopsin. One halothane docked in retinal pocket near tryptophan 265 (black licorice representation).

Table 2. Experimental and Calculated $\Delta G_{binding}$ for Select Proteins

		ΔG (kcal/mol)		
protein	VA	predicted	observed	rmsd (Å)
ketosteroid isomerase[8]	halothane	−3.27	−3.68	
		−3.40		
		−3.64	−4.15	
		−3.99	−3.98	
		−3.99	−3.98	
apoferritin[7]	halothane	−3.39	−6.17	3.6
	isoflurane	−3.27	−5.59	4.0
odorant binding protein[28]	halothane	−3.85	−4.55	
myoglobin[29]	halothane	−3.27	−3.13	
rhodopsin[31]	halothane	−3.81	−3.60	
calmodulin[2]	halothane	−3.13	−4.03	

binding proteins. This supports the underlying assumption that VA bind to pre-existing pockets in a protein structure

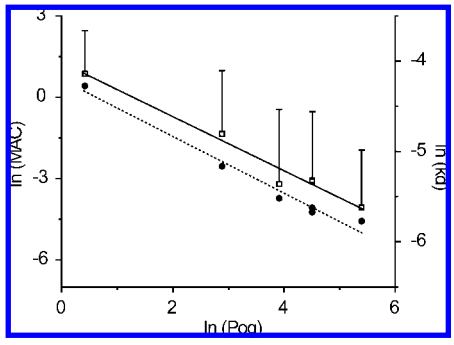

Figure 4. Plot of ln (MAC) (closed circles) and the mean (+sd) of the ln (kd) (open squares) versus ln (Pog) for the various VA. The ln (MAC) values are scaled to the left ordinate, and the mean ln (kd) values are scaled to the right ordinate. The solid and dotted lines are linear fits to the ln (kd) and ln (MAC) data, respectively.

that exceed the parameters of solvent exclusion and aliphaticity quantified by the modified PASS algorithm. These 41 structures include three for which the binding of VA, determined by halothane cross-linking, is matrix dependent. In addition, BSP were found in structures of 1 of the 2 proteins to which halothane cross-linking was not observed. Thus there is a good but not perfect correlation between BSP in a protein structure and VA binding. Possible explanations for the imperfect correlation between the PASS algorithm and halothane cross-linking studies include the following: the algorithm misidentifies some amphiphilic pockets as BSP while overlooking others; some VA binding sites yield false negatives because of low cross-linking efficiencies due to the protein sequence; and the structures of some proteins are different *in vitro* due to changes in the protein conformation resulting from covalent modifications or interactions with ligands or proteins, all of which may depend on the cellular milieus.

We found that the location of the BSP agreed with the actual VA binding pockets in 6 of 7 proteins with experimental evidence to resolve binding location. The lone exception being the putative halothane binding site in adenylate kinase. We cannot explain this discrepancy because the coordinates of the original structure are not available for analysis. These findings further support using the modified PASS algorithm to define BSP in protein structures.

VA-protein binding is consistently found to have an enthalpically favorable component, which indicates that VA ligands participate in VDW, hydrogen bonding, and electrostatic interactions with proteins.[18,32] These interactions do not strongly favor VA-protein association because they can be similar in magnitude to interactions with solvent molecules at the same sites,[33] hence the relatively low affinity of VA-protein complexes. However, several characteristics of buried

amphiphilic pockets may contribute to the thermodynamic favorability of VA-protein association. First, methyl groups provide abundant favorable VDW contacts and limit the number of strong hydrogen bonding and electrostatic interactions. This allows for potential enthalpic gain if water molecules displaced by the VA ligand are better able to satisfy their hydrogen bonding potential in the bulk than in the pocket.[18,33] Second, a limited number of water molecules in the BSP may promote VA binding. Water molecules that occupy space otherwise unfilled by the VA ligand maintain the integrity of the pocket while allowing a range in the size of VA molecules that bind.[18] In addition, any water molecules that remain in the pocket and associate with the VA ligand will diminish the unfavorable enthalpy of VA solvation.[34] Third, methyl groups might act as weak hydrogen bond donors that interact with the fluorine acceptors on the VA molecules.[35] We found that fluorine atoms on isoflurane and halothane ligands are within 2.1−2.5 Å of methyl hydrogen atoms on LEU 24 and LEU 81 of apoferritin (1XZ1 and 1XZ3) and fluorine atoms on a halothane ligand are within 2.2−2.4 Å of methyl hydrogen atoms on VAL 433 and LEU 453 of HSA (1E7B). These distances may indicate weak hydrogen bonding interactions in VA-protein complexes that augment those noted by others.[18] Together these may explain why VA binding sites correlate with the solvent exclusion and methyl group content quantified in the modified PASS algorithm.

We found that the calculated $\Delta G_{binding}$ values are consistent with most but not all observed dissociation constants. Consistency is defined as a calculated and observed $\Delta G_{binding}$ value that are within 2.5 kcal/mol, which is the standard deviation between the predicted and observed $\Delta G_{binding}$ values for a set of ligand-protein complexes with kds that span several orders of magnitude.[23] A concern is that small differences in the $\Delta G_{binding}$ values of the various VA may be obscured by the standard deviation of the algorithm because the VA potencies span a narrow continuum. However, the VA molecules studied are similar in size and formula yet have varying potencies, and the topology files were generated using the same method (PRODRG). For these molecules, the effects on $\Delta G_{binding}$ due to errors in the parametrization of the topology files, AMBER force field, or Autodock3 free energy function should be similar. When docked to the same site, errors between the calculated and observed $\Delta G_{binding}$ values should be of the same sign and approximate magnitude, which should preserve the relative ranking of the VA $\Delta G_{binding}$ values and hence slope of ln (kd) vs ln (Pog). Indeed, the differences between the calculated $\Delta G_{binding}$ values of the various VA, which average less than 0.9 kcal/mol, are consistent from BSP to BSP, and the $\Delta G_{binding}$ values of halothane and isoflurane are lower than for the corresponding lower-potency analogs.

The differences in the $\Delta G_{binding}$ values between the various VA molecules docked within a particular pocket are due mainly to differences in VDW contacts. This is apparent when comparing the nearly identical $\Delta G_{binding}$ values of the isomers. The topology files of the (R) and (S) isomers of either halothane or isoflurane differ only in the spatial charge distribution (dipole moment) and hence the ΔG_{tor} and ΔG_{hbond} terms are identical and the ΔG_{vdw}, ΔG_{elec}, and ΔG_{sol} terms are similar. On the other hand, the significant differences between the $\Delta G_{binding}$ values of NHL and halothane are about twice that of NFL and isoflurane. NHL differs from halothane by two fluorine atoms that replace a Br and a Cl atom. NFL differs from isoflurane by a Fl atom that replaces a Cl atom. In both cases, the fluorine atom has a smaller VDW radius than the halogen it replaces on the corresponding clinical VA with higher potency. These substitutions do not affect the number of torsions or the number of hydrogen bond donor/acceptors parametrized by Autodock so the ΔG_{tor} and ΔG_{hbond} terms are identical. As we noted for the isomers, differences in the spatial distribution of the partial charges have minimal effect on the ΔG_{vdw}, ΔG_{elec}, and ΔG_{sol} terms. Thus the significant differences between the $\Delta G_{binding}$ values of the clinical VA and lower potency analogs are due to VDW interactions. This suggests that VDW contacts are sufficient to predict the Meyer-Overton rule for these VA; however, the ΔG_{vdw} term may compensate for weak hydrogen bonding interactions not directly parametrized in the ΔG_{hbond} of Autodock.[23]

The BSP and $\Delta G_{binding}$ values for ketosteroid isomerase are consistent with the results of a prior docking study carried out with Autodock3 and supported by NMR experiments.[8] The two studies yield similar results despite the methods differing in two important ways. First, the agreement between the $\Delta G_{binding}$ values calculated in this work and the previous study indicate that topology files for VA molecules derived with PRODRG yield results consistent with those determined *ab initio*.[36] Second, the consistency in the locations of the predicted binding sites between the two methods indicates that the use of PASS to narrow the search area of the docking to amphiphilic pockets is as accurate as a blind docking approach[37] and is a more efficient method, especially when docking multiple VA protein combinations.

The modified PASS algorithm accurately identified the single BSP at the apoferritin dimer interface. However, the rmsd between the coordinates of halothane and isoflurane in the crystal structures and their docked location was 3.6 and 4.0 Å, respectively. This is approximately twice that which is considered acceptable when reproducing a known structure of a protein−ligand complex. Some error is introduced because the rmsd is calculated between the coordinates of the ligands docked into the structure of 1AEW and the coordinates of the ligands determined in the structures of 1XZ1 and 1XZ3. Even though VA do not induce significant changes in the protein structure, the alignment of 1AEW with either 1XZ1 or 1XZ3 is imperfect due to subtle differences throughout (Figure 3). However, no single set of ligand coordinates in the binding site can capture all of the molecular interactions since VA are in fast exchange[38] and have relatively short lifetimes in the binding site.[39] The calculated $\Delta G_{binding}$ of halothane and isoflurane are also not consistent with the experimental values. The high rmsd and inconsistency of the predicted $\Delta G_{binding}$ value of the docked and observed VA ligands suggest that other forces, in addition to VDW, contribute significantly to the binding energy. These additional forces might include weak hydrogen bonding to the halogen constituents of the VA molecules, which are not incorporated in the free energy function, or solvation forces, which might be better handled using a free energy perturbation method. The accuracy in the calculated binding energy of halothane binding to the four α helix bundle domain of rhodopsin, which is buried in lipid bilayer, may favor the latter explanation.

Halothane binds in the retinal pocket near W265 of rhodopsin with a $\Delta G_{binding}$ that is consistent with the value determined by intrinsic tryptophan quenching. The other three predicted sites are on the intracellular surface of the receptor near the lipid aqueous protein interface in domains which may be modified by interactions with other proteins, such as heterotrimeric G proteins. These results are consistent with experimental evidence that indicates multiple halothane binding sites in rhodopsin, including the retinal pocket where [^{14}C]halothane cross-links to W265.[31] These results suggest that the affinity of halothane for the retinal pocket, which is submerged in the lipid bilayer, is not affected by the lipid in a way that cannot be accounted for with our method.

The complexes of VA with apoferritin and rhodopsin demonstrate VA binding to 4 α helix bundle motifs, such as those found within the transmembrane domains of anesthetic sensitive members of the cys-loop superfamily of ion channels that include NAChR, GABA-A, and glycine receptors.[40] Photoaffinity labeling experiments indicate numerous halothane binding sites spread throughout the various NAChR subunits.[41] Mutagenesis studies on GABA-A and glycine receptors indentified certain residues, which abolish anesthetic sensitivity when substituted for with larger amino acids that have fewer methyl groups.[42,43] These findings suggest that anesthetic sensitivity could result from binding to discrete site(s), which can be occluded or altered to have lower anesthetic affinity. This view is supported by the structures of VA complexes with apoferritin and rhodopsin, which also serve as models of VA binding to the transmembrane domains of GABA-A and glycine receptor subunits until they are determined experimentally.

Adenylate kinase was the first VA-protein complex to have the structure determined. The structure was inferred from a difference-Fourier map of nucleotide free porcine adenylate kinase soaked in a saturated solution of halothane minus nucleotide free adenylate kinase.[30] A single halothane molecule was assigned to electron density in the difference map based on approximate volume. The authors concluded that the halothane was located within a pocket between residues 11−28, 91, 116−118, and 18 where the adenine moiety of AMP also binds. In this work, we used the crystal structure of nucleotide free porcine adenylate kinase determined subsequently by other workers (3ADK). It was immediately apparent that 3ADK lacked a pocket with sufficient volume to accommodate a VA molecule near the putative halothane binding site. This suggests that VA binding induces a structural change in adenylate kinase, a phenomenon that has not been observed in any other VA-protein complex. Neither of the two BSP identified by our approach were within the residues that lined the putative halothane site because our approach explicitly assumes that VA molecules bind to existing pockets. However, one of the VA BSP determined in our approach is located in the corresponding AMP binding site in the homologous structure of adenylate kinase from *E. coli*, determined with ADP and AMP ligands (2ECK). Thus our finding that VA bind near the AMP site is consistent with the conclusions of the original structure of adenylate kinase-halothane complex, yet there is disagreement as to the internal coordinates of this site.

In conclusion, VA bind to amphiphilic pockets with high solvent exclusion and aliphatic character. The water molecules in the VA binding sites maintain pocket integrity and diminish unfavorable solvation of the VA. The aliphatic residues in the VA binding sites provide favorable VDW contacts and weak hydrogen bond donors. VA docked to these pockets have $\Delta G_{binding}$ values that trend according to the Meyer-Overton rule. The binding of these VA is primarily driven by VDW interactions. Weak hydrogen bonding and electrostatic interactions make minor contributions to VA binding.

ACKNOWLEDGMENT

This study was supported in part by grants GM070585 and HL-45532 from the National Institutes of Health, Bethesda, MD.

Supporting Information Available: Details of protein structures (Table S1). This material is available free of charge via the Internet at http://pubs.acs.org.

REFERENCES AND NOTES

(1) Franks, N. P.; Lieb, W. R. Do general anaesthetics act by competitive binding to specific receptors. *Nature* **1984**, *310* (5978), 599–601.
(2) Streiff, J. H.; Allen, T. W.; Atanasova, E.; Juranic, N.; Macura, S.; Penheiter, A. R.; Jones, K. A. Prediction of volatile anesthetic binding sites in proteins. *Biophys. J.* **2006**, *91* (9), 3405–14.
(3) Woo, H. J. Calculation of absolute protein-ligand binding constants with the molecular dynamics free energy perturbation method. *Methods Mol. Biol.* **2008**, *443*, 109–20.
(4) Chen, Y. Z.; Zhi, D. G. Ligand-protein inverse docking and its potential use in the computer search of protein targets of a small molecule. *Proteins* **2001**, *43* (2), 217–26.
(5) Bhattacharya, A. A.; Curry, S.; Franks, N. P. Binding of the general anesthetics propofol and halothane to human serum albumin. High resolution crystal structures. *J. Biol. Chem.* **2000**, *275* (49), 38731–8.
(6) Franks, N. P.; Jenkins, A.; Conti, E.; Lieb, W. R.; Brick, P. Structural basis for the inhibition of firefly luciferase by a general anesthetic. *Biophys. J.* **1998**, *75* (5), 2205–11.
(7) Liu, R.; Loll, P. J.; Eckenhoff, R. G. Structural basis for high-affinity volatile anesthetic binding in a natural 4-helix bundle protein. *FASEB J.* **2005**, *19* (6), 567–76.
(8) Yonkunas, M. J.; Xu, Y.; Tang, P. Anesthetic interaction with ketosteroid isomerase: insights from molecular dynamics simulations. *Biophys. J.* **2005**, *89* (4), 2350–6.
(9) Szarecka, A.; Xu, Y.; Tang, P., Dynamics of Firefly Luciferase Inhibition by General Anesthetics: Gaussian and Anisotropic Network Analyses. Biophys. J. 2007.
(10) Eckenhoff, R. G.; Johansson, J. S. Molecular interactions between inhaled anesthetics and proteins. *Pharmacol. Rev.* **1997**, *49* (4), 343–67.
(11) Pan, J. Z.; Xi, J.; Tobias, J. W.; Eckenhoff, M. F.; Eckenhoff, R. G. Halothane binding proteome in human brain cortex. *J. Proteome Res.* **2007**, *6* (2), 582–92.
(12) Xi, J.; Liu, R.; Asbury, G. R.; Eckenhoff, M. F.; Eckenhoff, R. G. Inhalational anesthetic-binding proteins in rat neuronal membranes. *J. Biol. Chem.* **2004**, *279* (19), 19628–33.
(13) Humphrey, W.; Dalke, A.; Schulten, K. VMD: visual molecular dynamics. *J. Mol. Graphics Modell.* **1996**, *14* (1), 33−827−8.
(14) Phillips, J. C.; Braun, R.; Wang, W.; Gumbart, J.; Tajkhorshid, E.; Villa, E.; Chipot, C.; Skeel, R. D.; Kale, L.; Schulten, K. Scalable molecular dynamics with NAMD. *J. Comput. Chem.* **2005**, *26* (16), 1781–802.
(15) Brady, G. P., Jr.; Stouten, P. F. Fast prediction and visualization of protein binding pockets with PASS. *J. Comput.-Aided Mol. Des.* **2000**, *14* (4), 383–401.
(16) Shikii, K.; Sakurai, S.; Utsumi, H.; Seki, H.; Tashiro, M. Application of the 19F NMR technique to observe binding of the general anesthetic halothane to human serum albumin. *Anal. Sci.* **2004**, *20* (10), 1475–7.
(17) Yokono, S.; Ogli, K.; Miura, S.; Ueda, I. 400 MHz two-dimensional nuclear Overhauser spectroscopy on anesthetic interaction with lipid bilayer. *Biochim. Biophys. Acta* **1989**, *982* (2), 300–2.
(18) Bertaccini, E. J.; Trudell, J. R.; Franks, N. P. The common chemical motifs within anesthetic binding sites. *Anesth. Analg. (Baltimore)* **2007**, *104* (2), 318–24.
(19) Eger, E. I., 2nd.; Koblin, D. D.; Laster, M. J.; Schurig, V.; Juza, M.; Ionescu, P.; Gong, D. Minimum alveolar anesthetic concentration

values for the enantiomers of isoflurane differ minimally. *Anesth. Analg. (Baltimore)* **1997**, *85* (1), 188–92.
(20) Xu, Y.; Tang, P.; Firestone, L.; Zhang, T. T. 19F nuclear magnetic resonance investigation of stereoselective binding of isoflurane to bovine serum albumin. *Biophys. J.* **1996**, *70* (1), 532–8.
(21) van Aalten, D. M.; Bywater, R.; Findlay, J. B.; Hendlich, M.; Hooft, R. W.; Vriend, G. PRODRG, a program for generating molecular topologies and unique molecular descriptors from coordinates of small molecules. *J. Comput.-Aided Mol. Des.* **1996**, *10* (3), 255–62.
(22) Schuttelkopf, A. W.; van Aalten, D. M. PRODRG: a tool for high-throughput crystallography of protein-ligand complexes. *Acta Crystallogr., Sect. D: Biol. Crystallogr.* **2004**, *60* (Pt 8), 1355–63.
(23) Morris, G. M.; Goodsell, D. S.; Halliday, R. S.; Huey, R.; Hart, W. E.; Belew, R. K.; Olson, A. J. Automated Docking Using a Lamarckian Genetic Algorithm and an Empirical Binding Free Energy Function. *J. Comput. Chem.* **1998**, *19* (14), 1639–1662.
(24) Weiner, S. J.; Kollman, P. A.; Case, D. A.; Singh, U. C.; Ghio, C.; Alagona, G.; Profeta, S.; Weiner, P. A new force field for molecular mechanical simulation of nucleic acids and proteins. *J. Am. Chem. Soc.* **1984**, *106* (3), 765–784.
(25) Sanner, M. F. Python: a programming language for software integration and development. *J. Mol. Graphics Modell.* **1999**, *17* (1), 57–61.
(26) Vaque, M.; Arola, A.; Aliagas, C.; Pujadas, G. BDT: an easy-to-use front-end application for automation of massive docking tasks and complex docking strategies with AutoDock. *Bioinformatics* **2006**, *22* (14), 1803–4.
(27) Phillips, J. C.; Wriggers, W.; Li, Z.; Jonas, A.; Schulten, K. Predicting the structure of apolipoprotein A-I in reconstituted high-density lipoprotein disks. *Biophys. J.* **1997**, *73* (5), 2337–46.
(28) Johansson, J. S.; Manderson, G. A.; Ramoni, R.; Grolli, S.; Eckenhoff, R. G. Binding of the volatile general anesthetics halothane and isoflurane to a mammalian beta-barrel protein. *FEBS J.* **2005**, *272* (2), 573–81.
(29) Eckenhoff, R. G.; Pidikiti, R.; Reddy, K. S. Anesthetic stabilization of protein intermediates: myoglobin and halothane. *Biochemistry* **2001**, *40* (36), 10819–24.
(30) Sachsenheimer, W.; Pai, E. F.; Schulz, G. E.; Schirmer, R. H. Halothane binds in the adenine-specific niche of crystalline adenylate kinase. *FEBS Lett.* **1977**, *79* (2), 310–2.
(31) Ishizawa, Y.; Pidikiti, R.; Liebman, P. A.; Eckenhoff, R. G. G protein-coupled receptors as direct targets of inhaled anesthetics. *Mol. Pharmacol.* **2002**, *61* (5), 945–52.
(32) Sawas, A. H.; Pentyala, S. N.; Rebecchi, M. J. Binding of volatile anesthetics to serum albumin: measurements of enthalpy and solvent contributions. *Biochemistry* **2004**, *43* (39), 12675–85.
(33) Barratt, E.; Bingham, R. J.; Warner, D. J.; Laughton, C. A.; Phillips, S. E.; Homans, S. W. Van der Waals interactions dominate ligand-protein association in a protein binding site occluded from solvent water. *J. Am. Chem. Soc.* **2005**, *127* (33), 11827–34.
(34) Luque, I.; Freire, E. Structural parameterization of the binding enthalpy of small ligands. *Proteins* **2002**, *49* (2), 181–90.
(35) Kryachko, E.; Scheiner, S. CH-F Hydrogen Bonds, Dimers of Fluoromethanes. *J. Phys. Chem. A* **2004**, *108*, 2527–2535.
(36) Tang, P.; Zubryzcki, I.; Xu, Y. Ab Initio Calculation of structures and properties of halogenated general anesthetics: halothane and sevoflurane. *J. Comput. Chem.* **2001**, *22* (4), 436–444.
(37) Hetenyi, C.; van der Spoel, D. Efficient docking of peptides to proteins without prior knowledge of the binding site. *Protein Sci.* **2002**, *11* (7), 1729–37.
(38) Streiff, J. H.; Juranic, N. O.; Macura, S. I.; Warner, D. O.; Jones, K. A.; Perkins, W. J. Saturation transfer difference nuclear magnetic resonance spectroscopy as a method for screening proteins for anesthetic binding. *Mol. Pharmacol.* **2004**, *66*, 929–35.
(39) Dubois, B. W.; Evers, A. S. 19F-NMR spin-spin relaxation (T2) method for characterizing volatile anesthetic binding to proteins. Analysis of isoflurane binding to serum albumin. *Biochemistry* **1992**, *31* (31), 7069–76.
(40) Unwin, N. Refined structure of the nicotinic acetylcholine receptor at 4A resolution. *J. Mol. Biol.* **2005**, *346* (4), 967–89.
(41) Chiara, D. C.; Dangott, L. J.; Eckenhoff, R. G.; Cohen, J. B. Identification of nicotinic acetylcholine receptor amino acids photolabeled by the volatile anesthetic halothane. *Biochemistry* **2003**, *42* (46), 13457–67.
(42) Jenkins, A.; Greenblatt, E. P.; Faulkner, H. J.; Bertaccini, E.; Light, A.; Lin, A.; Andreasen, A.; Viner, A.; Trudell, J. R.; Harrison, N. L. Evidence for a common binding cavity for three general anesthetics within the GABAA receptor. *J. Neurosci.* **2001**, *21* (6), RC136.
(43) Mihic, S. J.; Ye, Q.; Wick, M. J.; Koltchine, V. V.; Krasowski, M. D.; Finn, S. E.; Mascia, M. P.; Valenzuela, C. F.; Hanson, K. K.; Greenblatt, E. P.; Harris, R. A.; Harrison, N. L. Sites of alcohol and volatile anaesthetic action on GABA(A) and glycine receptors. *Nature* **1997**, *389* (6649), 385–9.
(44) Franks, N. P.; Lieb, W. R. Temperature dependence of the potency of volatile general anesthetics: implications for in vitro experiments. *Anesthesiology* **1996**, *84* (3), 716–20.
(45) Eger, E. I., II.; Liu, J.; Koblin, D. D.; Laster, M. J.; Taheri, S.; Halsey, M. J.; Ionescu, P.; Chortkoff, B. S.; Hudlicky, T. Molecular properties of the "ideal" inhaled anesthetic: studies of fluorinated methanes, ethanes, propanes, and butanes. *Anesth. Analg. (Baltimore)* **1994**, *79* (2), 245–51.
(46) Koblin, D. D.; Laster, M. J.; Ionescu, P.; Gong, D.; Eger, E. I., 2nd.; Halsey, M. J.; Hudlicky, T. Polyhalogenated methyl ethyl ethers: solubilities and anesthetic properties. *Anesth. Analg. (Baltimore)* **1999**, *88* (5), 1161–7.

CI800206A